Statistical Characteristics of the Global Surface Current Speeds Obtained From Satellite Altimetry and Scatterometer Data

Peter C. Chu

***Abstract*—Near-real time ocean surface currents derived from satellite altimeter (JASON-1, GFO, ENVISAT) and scatterometer (QSCAT) data on $1^\circ \times 1^\circ$ resolution for world oceans (60° S to 60° N) are available online as "Ocean Surface Current Analyses-Real Time (OSCAR)." The probability distribution function (PDF) of the current speeds (w), constructed from global OSCAR data from 1992 to 2008, satisfies the two-parameter Weibull distribution reasonably well, and such a PDF has little seasonal and interannual variations. Knowledge on PDF of w will improve the ensemble horizontal flux calculation, which contributes to the climate studies.**

***Index Terms*—Altimetry, probability, satellites, scattering, sea surface, stochastic processes.**

I. Introduction

THE world oceans contribute significantly to the global redistribution of heat necessary to maintain the earth's thermal equilibrium. Surface layer horizontal fluxes of momentum, heat, water mass, and chemical constituents are typically nonlinear in the speed of horizontal currents [1], [2], so the space or time average flux is not generally equal to the flux that would be diagnosed from the averaged current speed. In fact, the average flux will generally depend on higher-order moments of the current speed, such as the standard deviation, skewness, and kurtosis. From both diagnostic and modeling perspectives, there is a need for parameterizations of the probability distribution function (PDF) of the current speed w (called w-PDF here).

Recent study on the equatorial Pacific [3] showed that the w-PDF satisfies the two-parameter Weibull distribution in the upper layer after analyzing the hourly acoustic Doppler current profiler (ADCP) data (1990–2007) at all the six stations along during the tropical atmosphere ocean (TAO) project. A question arises: Can such a result (e.g., the Weibull distribution for the equatorial Pacific surface current speeds) be extended to global oceans? To answer this question, we use the five-day ocean surface currents analyses-real-time (OSCAR) data to construct the observational w-PDF for the global ocean surface circulation. Special characteristics of the statistical parameters such as mean, standard deviation, skewness, and kurtosis will also be identified.

Manuscript received August 14, 2008; revised November 30, 2008. First published February 27, 2009; current version published April 29, 2009. This work was supported in part by the Office of Naval Research, in part by the Naval Oceanographic Office, and in part by the Naval Postgraduate School.

The author is with the Department of Oceanography, Naval Postgraduate School, Monterey, CA 93943 USA (e-mail: pcchu@nps.edu; p_c_chu@yahoo.com).

Color versions of one or more of the figures in this paper are available online at http://ieeexplore.ieee.org.

Digital Object Identifier 10.1109/JSTARS.2009.2014474

II. OSCAR Data

The OSCAR data are available for the world oceans from 60° N to 60° S on $1^\circ \times 1^\circ$ grid to a broad-based user community via a web-based interactive data selection interface on a time base with exactly 72 steps per year (about a five-day interval) starting from October 1992 (Fig. 1). The velocity is automatically computed from gridded fields of surface topography and wind derived on the base of the Ekman dynamics from satellite altimeter (JASON-1, GFO, ENVISAT) and scatterometer (QSCAT) vector wind data. See http://www.oscar.noaa.gov/ for detailed information.

III. Stochastic Differential Equations for Surface Currents

Let (x, y) be the horizontal coordinates and z be the vertical coordinate. Vertically averaged and linearized horizontal velocity components (u, v) from the surface to a constant scale depth (h) of surface mixed layer are given by [3]

$$\frac{\partial u}{\partial t} = \frac{1}{h}\Lambda_u - \frac{K}{h^2}u \tag{1}$$

$$\frac{\partial v}{\partial t} = \frac{1}{h}\Lambda_v - \frac{K}{h^2}v \tag{2}$$

where

$$\Lambda_u \equiv fV_E + \frac{\tau_x}{\rho}, \quad \Lambda_v \equiv -fU_E + \frac{\tau_y}{\rho} \tag{3}$$

represent the residual between the Ekman transport and surface wind stress. Here, K is the Rayleigh friction coefficient; f is the Coriolis parameter; (τ_x, τ_y) are the surface wind stress components; h is the Ekman depth; and (U_E, V_E) are Ekman transports computed by

$$(U_E, V_E) = \int_{-h}^{0} (\tilde{u} - u_g, \tilde{v} - v_g)dz \tag{4}$$

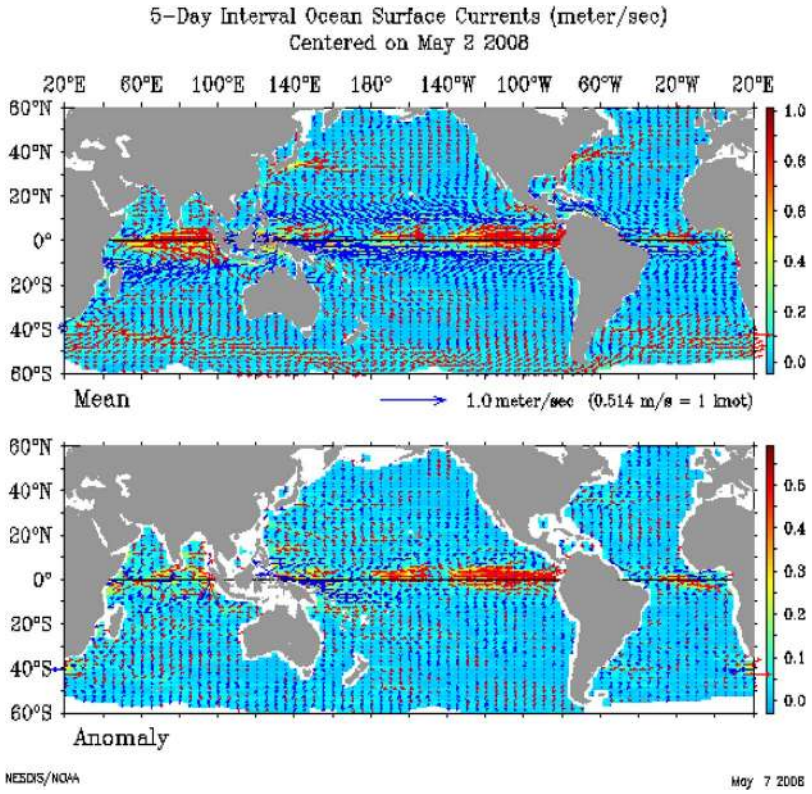

Fig. 1. Global ocean surface current vectors (five-day mean and anomaly) derived from satellite altimeter and scatterometer data. The data can be downloaded from the website: http://www.oscar.noaa.gov/.

where $(\tilde{u}, \tilde{v})$ are the vertically varying horizontal velocity components and (u_g, v_g) are the geostrophic velocity components

$$u_g = -\frac{1}{f\rho}\frac{\partial p}{\partial y}, \quad v_g = \frac{1}{f\rho}\frac{\partial p}{\partial x}.$$

Here, p is the pressure. With absence of horizontal pressure gradient, e.g., $u_g = v_g = 0$, (1) and (2) reduce to the commonly used wind-forced slab model [4]. For the sake of convenience, we assume that the residual between the Ekman transports (U_E, V_E) and surface wind stress does not depend on the horizontal current vector (u, v). Away from the equator, this approximation is similar to a small Rossby number approximation [5]. If the forcing (Λ_u, Λ_v) is fluctuating around some mean value

$$\Lambda_u(t) = \langle \Lambda_u \rangle + \dot{W}_1(t)h\Sigma, \quad \Lambda_v(t) = \langle \Lambda_v \rangle + \dot{W}_2(t)h\Sigma \quad (5)$$

where the angle brackets represent ensemble mean and the fluctuations are taken to be isotropic and white in time

$$\left\langle \dot{W}_i(t_1)\dot{W}_j(t_2) \right\rangle = \delta_{ij}\delta(t_1 - t_2) \quad (6)$$

with a strength that is represented by Σ. Note that the Ekman transport is determined by the surface wind stress for time-independent case and, therefore, the ensemble mean values of (Λ_u, Λ_v) are zero

$$\langle \Lambda_u \rangle = 0, \quad \langle \Lambda_v \rangle = 0. \quad (7)$$

Substitution of (5)–(7) into (1) and (2) gives

$$\frac{\partial u}{\partial t} = -\frac{K}{h^2}u + \dot{W}_1(t)\Sigma \quad (8)$$

$$\frac{\partial v}{\partial t} = -\frac{K}{h^2}v + \dot{W}_2(t)\Sigma \quad (9)$$

which is a set of stochastic differential equations for the surface current vector. The joint PDF of (u, v) satisfies the Fokker–Planck equation

$$\frac{\partial p}{\partial t} = \left(\frac{\Sigma^2}{2}\right)\left(\frac{\partial^2 p}{\partial u^2} + \frac{\partial^2 p}{\partial v^2}\right) + \frac{\partial}{\partial u}\left[\left(\frac{K}{h^2}u\right)p\right] + \frac{\partial}{\partial v}\left[\left(\frac{K}{h^2}v\right)p\right] \quad (10)$$

which is a linear second-order partial differential equation with the depth scale (h) taken as a constant. The orthogonal coordinates (u, v) are transformed into the polar coordinates (w, φ)

$$u = w\cos\varphi, \quad v = w\sin\varphi \quad (11)$$

with w the current speed and φ the direction. The joint PDF of (u, v) is changed into the joint PDF of (w, φ)

$$p(u, v)dudv = p(u, v)wdwd\varphi = \tilde{p}(w, \varphi)dwd\varphi. \quad (12)$$

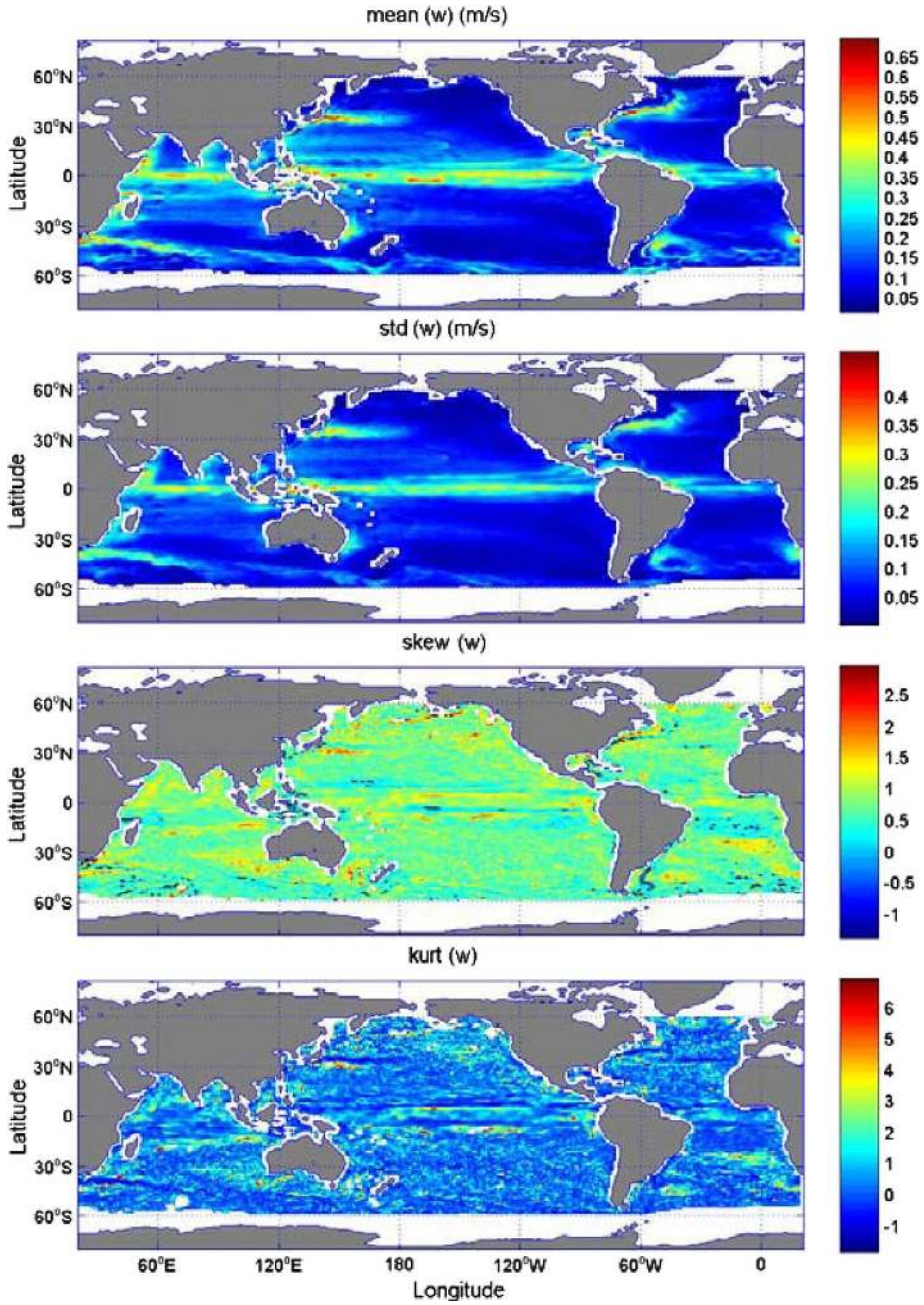

Fig. 2. First four parameters of the surface current speeds calculated from the OSCAR data (1992–2008).

Integration of (12) over the angle φ from 0 to 2π yields the marginal PDF for the current speed alone

$$p(w) = \int_0^{2\pi} \tilde{p}(w, \varphi) d\varphi. \tag{13}$$

For a constant Rayleigh friction coefficient (K) at $z = -h$, the steady state solution of (10) is given by

$$p(u, v) = A \exp\left[-\frac{K}{\Sigma^2 h^2}(u^2 + v^2)\right] \tag{14}$$

where A is a normalization constant. Substitution of (14) into (12) and use of (13) yield the Rayleigh distribution

$$p(w) = \frac{2w}{a^2} \exp\left[-\left(\frac{w}{a}\right)^2\right], \quad a \equiv \frac{\Sigma h}{\sqrt{K}} \tag{15}$$

with the scale parameter a. The basic postulation of constant K may not be met always at the upper ocean. Hence, we require a model that can meet the twin objectives of (a) accommodating Rayleigh distribution whenever the basic hypothesis (constant K) that justifies it is satisfied and (b) fitting data under more general conditions. This requirement is supposed to be satisfied by the Weibull probability density function

$$p(w) = \frac{b}{a}\left(\frac{w}{a}\right)^{b-1} \exp\left[-\left(\frac{w}{a}\right)^b\right] \tag{16}$$

where the parameters a and b denote the scale and shape of the distribution. This distribution has been recently used in investigating the ocean model predictability [6], [7].

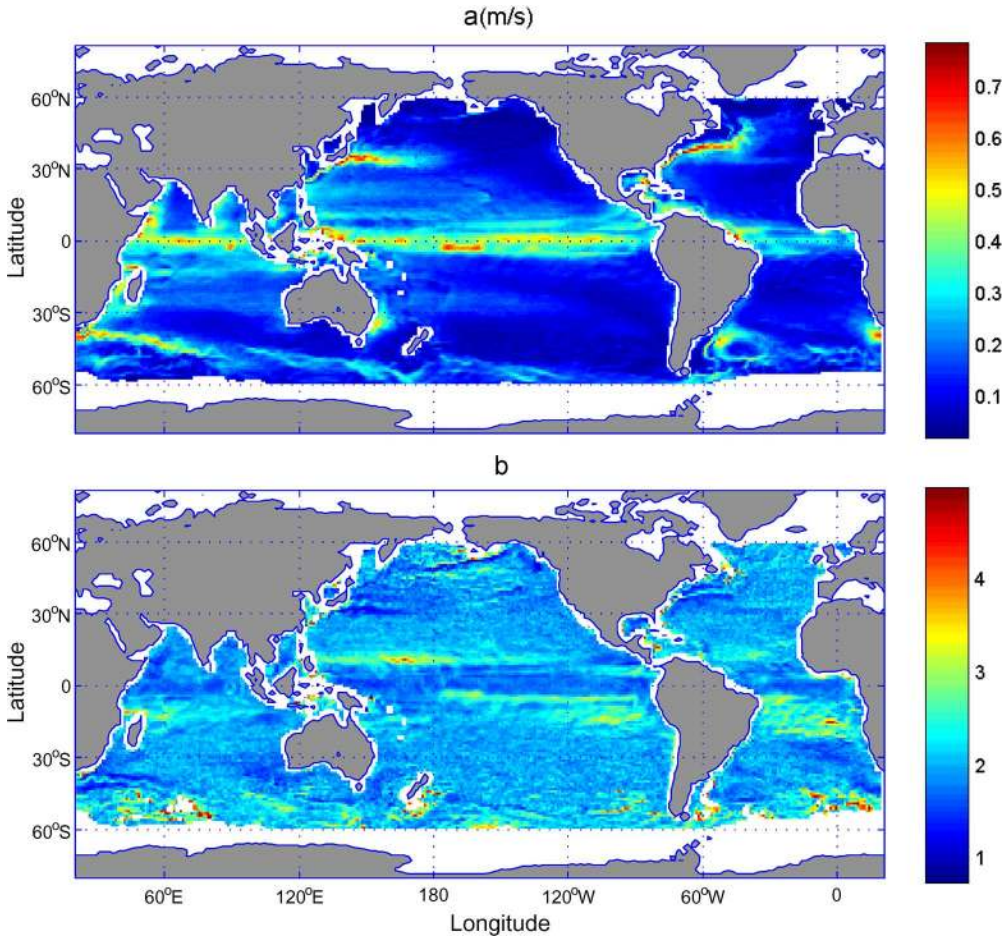

Fig. 3. Same as in Fig. 2, but for Weibull parameters (a, b).

IV. Parameters of the Weibull Distribution

The four parameters (mean μ, standard deviation σ, skewness γ_1, and kurtosis excess γ_2) of the Weibull distribution are calculated by [8]

$$\mu = a\Gamma\left(1+\frac{1}{b}\right) \tag{17}$$

$$\sigma^2 = a^2\Gamma\left(1+\frac{2}{b}\right) - \mu^2 \tag{18}$$

$$\gamma_1 = \frac{a^3\Gamma\left(1+\frac{3}{b}\right) - 3\mu\sigma^2 - \mu^3}{\sigma^3} \tag{19}$$

$$\gamma_2 = \frac{a^4\Gamma(1+4/b) - 4\gamma_1\sigma^3\mu - 6\mu^2\sigma^2 - \mu^4}{\sigma^4} \tag{20}$$

where Γ is the gamma function. The parameters a and b can be inverted [9] from (17) and (18)

$$b \simeq \left[\frac{\mu}{\sigma}\right]^{1.086}, \quad a = \frac{\mu}{\Gamma(1+1/b)}. \tag{21}$$

The skewness and excess kurtosis depend on the parameter b only [see (17)to (21)] for the Weibull distribution. The relationship between the kurtosis and skewness can be determined from (20) and (21).

V. Observational w-PDF

The data depicted in Section II are used to investigate the statistical features of the global surface current speeds (w). The four parameters (mean, standard deviation, skewness, and kurtosis excess) can also be calculated from the observational data (w)

$$\text{mean}(w) = \frac{1}{N}\sum_{i=1}^{N} w_i, \ \text{std}(w) = \sqrt{\text{mean}\left[w - \text{mean}(w)\right]^2}$$

$$\text{skew}(w) = \frac{\text{mean}\left\{\left[w - \text{mean}(w)\right]^3\right\}}{\text{std}^3(w)}$$

$$\text{kurt}(w) = \frac{\text{mean}\left\{\left[w - \text{mean}(w)\right]^4\right\}}{\text{std}^4(w)} - 3 \tag{22}$$

for the each grid point. The mean, standard deviation, skewness, and kurtosis fields of w estimated from the OSCAR data are displayed in Fig. 2. Large values of $\text{mean}(w)$ occur in the western boundaries such as in the Gulf Stream, Kuroshio, and Somali current, Malvinas current; secondary maxima in the equatorial zones especially in the western and central equatorial Pacific, and the Antarctic circumpolar current. The minima are found in the middle of the basins at mid-latitudes. The standard deviation of w is also large near the western boundaries and in the equatorial zones. In general, w is positively skewed in the most part

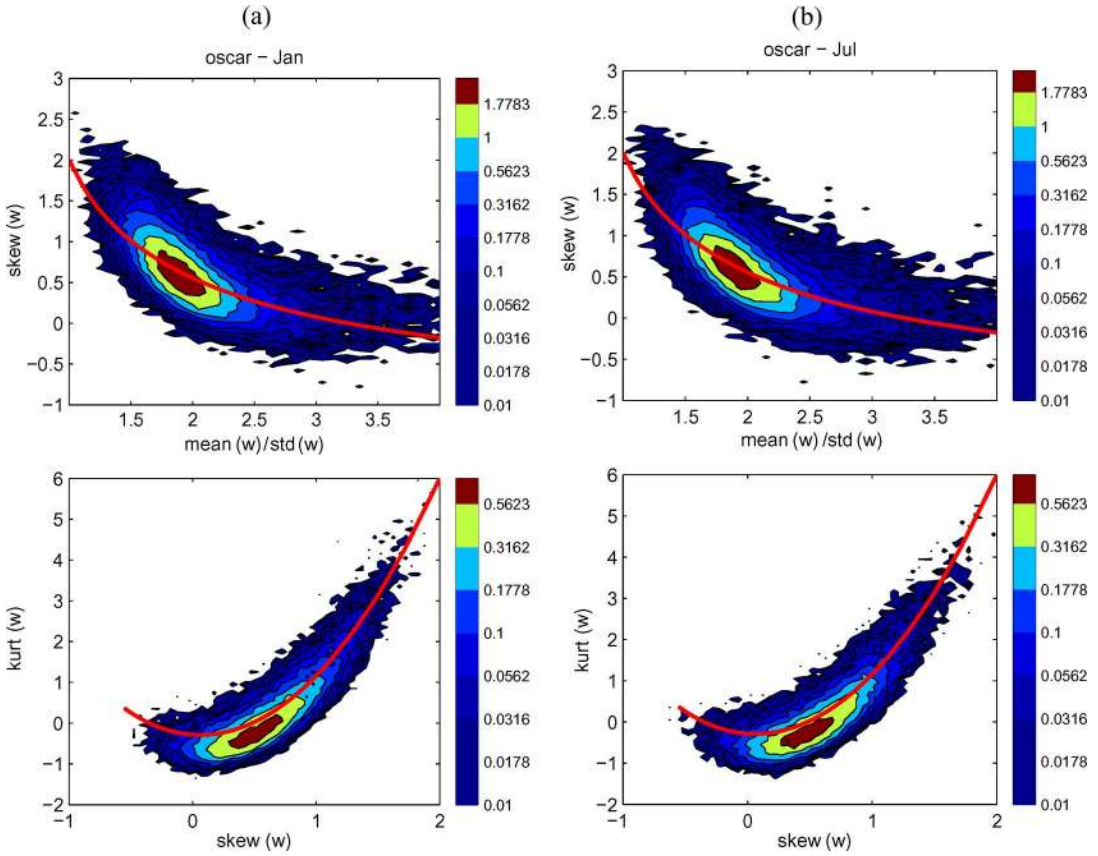

Fig. 4. Kernel density estimates of joint PDFs of (top) $\mathrm{mean}(w)/\mathrm{std}(w)$ and $\mathrm{skew}(w)$ and (bottom) $\mathrm{skew}(w)$ and $\mathrm{kurt}(w)$ for (left) for (a) January and (b) July OSCAR data from 1992 to 2008. The contour intervals are logarithmically spaced. The thick red line is the theoretical curve for a Weibull variable.

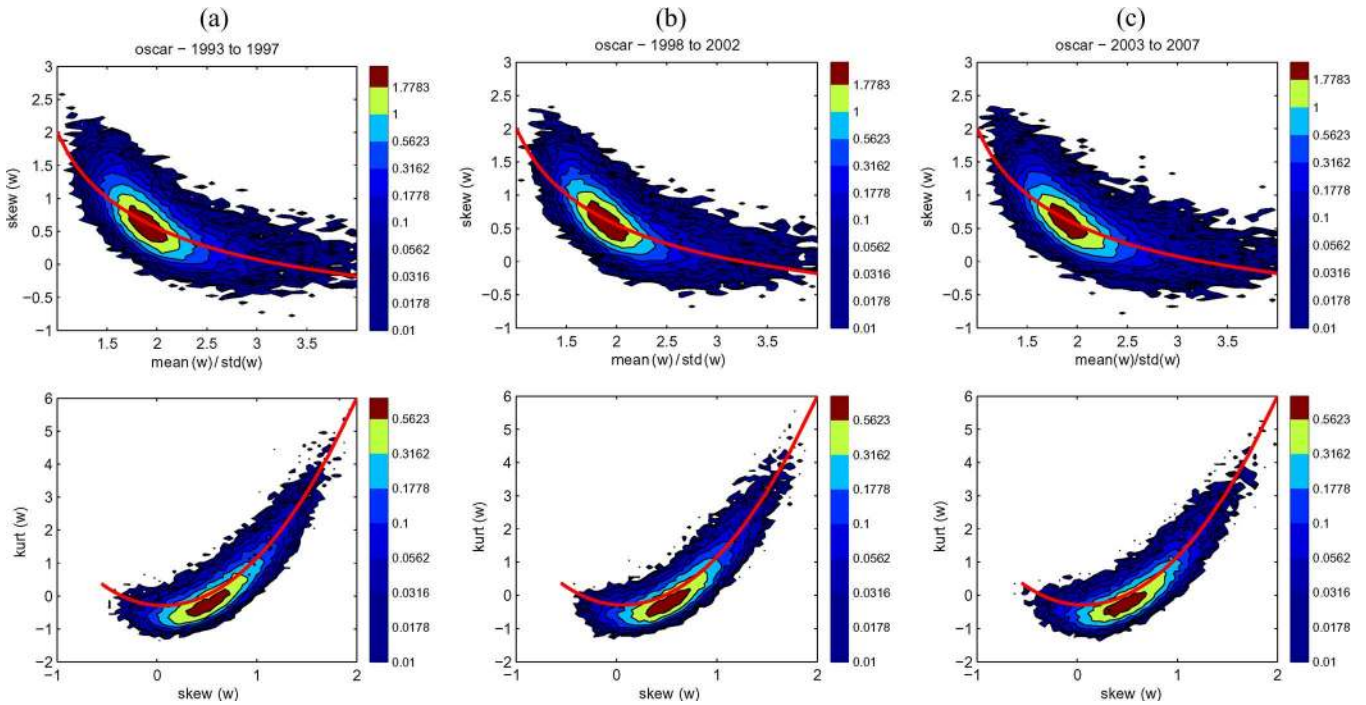

Fig. 5. Kernel density estimates of joint PDFs of (top) $\mathrm{mean}(w)/\mathrm{std}(w)$ and $\mathrm{skew}(w)$ and (bottom) $\mathrm{skew}(w)$ and $\mathrm{kurt}(w)$ for (left) from the OSCAR data during (a) 1993–1997, (b) 1998–2002, and (c) 2003–2007. The contour intervals are logarithmically spaced. The thick red line is the theoretical curve for a Weibull variable.

of the global oceans. The skewness is banded especially along the equator with an eddy structure along the boundary currents. The kurtosis excess field is much noisier than those of $\mathrm{mean}(w)$, $\mathrm{std}(w)$, or $\mathrm{skew}(w)$.

The Weibull parameters (a, b) were calculated by (21) from $\mathrm{mean}(w)$ and $\mathrm{std}(w)$. The distribution of the parameter a over the global oceans [Fig. 3(a)] is quite close to the distribution of $\mathrm{mean}(w)$, i.e., with large values in western boundaries and equatorial zone. The distribution of the Weibull parameter b is shown in Fig. 3(b). Thus, a four-parameter dataset (mean, std, skew, kurt) has been established each location.

The relationships between $\mathrm{skew}(w)$ and $\mathrm{mean}(w)/\mathrm{std}(w)$ and between the $\mathrm{kurt}(w)$ and the $\mathrm{skew}(w)$ may be used to identify the fitness of the Weibull distribution for observational w-PDFs. Fig. 4 shows the kernel density estimates of joint PDFs of $\mathrm{mean}(w)/\mathrm{std}(w)$ versus $\mathrm{skew}(w)$ and $\mathrm{kurt}(w)$ versus $\mathrm{skew}(w)$ for January (left panels) and July (right panels) OSCAR data from 1992–2008. Fig. 5 shows the similar items from the OSCAR data during (a) 1993–1997, (b) 1998–2002, and (c) 2003–2007. The contour intervals are logarithmically spaced. The thick red line is the theoretical curve for a Weibull variable. The corresponding Weibull variable has theoretical (γ_1, b) and (γ_2, γ_1) relationships, as represented by the solid curve in these figures.

For the observational surface current speeds (w), the $\mathrm{skew}(w)$ is evidently a concave function of the ratio $\mathrm{mean}(w)/\mathrm{std}(w)$ (the same as the Weibull distribution), such that the theoretical function is positive for small values of this ratio and negative for large values. However, for the core of the kernel with the joint probability higher than 0.32, mean(w)/std(w) is always less than 2.2 and $\mathrm{skew}(w)$ is always positive (Fig. 4, upper panes). Similarly, the relationship between $\mathrm{skew}(w)$ and $\mathrm{kurt}(w)$ in the observations is similar to that for a Weibull variable (Fig. 4, lower panels) with slightly smaller kurtosis excess. This shows the discrepancy between the Weibull model with observations. These features are almost the same between January [Fig. 4(a)] and July [Fig. 4(b)], and among three time periods: 1993–1997 [Fig. 5(a)], 1998–2002 [Fig. 5(b)], and 2003–2007 [Fig. 5(c)]. The agreement between the moment relationships in the OSCAR data and those for a Weibull variable reinforces the conclusion that these data are Weibull to a good approximation.

VI. Conclusion

This study has investigated the probability distribution function of the surface current speeds (w), using long-term (1992–2008) five-day OSCAR data and, theoretically, using a stochastic model derived using upper boundary layer physics. The following results were obtained.

1) Probability distribution function of the global surface current speeds (w) approximately satisfies the two-parameter Weibull distribution. For constant Rayleigh friction coefficient K, the probability distribution function satisfies a linear second-order partial differential equation (i.e., the Fokker–Planck equation) with an analytical solution—the Rayleigh distribution (special case of the two-parameter Weibull distribution).
2) Four moments of w (mean, standard deviation, skewness, kurtosis) have been characterized. It was found that the relationships between $\mathrm{mean}(w)/\mathrm{std}(w)$ and $\mathrm{skew}(w)$ and between $\mathrm{skew}(w)$ and $\mathrm{kurt}(w)$ from the data are in fairly well agreement with the theoretical Weibull distribution for the global ocean surface current speed from 1992 to 2008. The OSCAR data also show that the ratio $\mathrm{mean}(w)/\mathrm{std}(w)$ is generally less than 2.2, and the skewness is generally positive for the whole global oceans.
3) The Weibull distribution provides a good empirical approximation to the PDF of global ocean surface current speeds with little seasonal and interannual variations. This may improve the representation of the horizontal fluxes that are at the heart of the coupled physical-biogeochemical dynamics of the marine system.
4) Horizontal fluxes are significant in their nonglobal character, at the very least on a basin-wide scale. Regional differences of the four parameters (mean, std, skew, kurt) were found. However, the relationships between $\mathrm{mean}(w)/\mathrm{std}(w)$ and $\mathrm{skew}(w)$ and between $\mathrm{skew}(w)$ and $\mathrm{kurt}(w)$ were kept the same. This indicates that the Weibull distribution is valid for the global oceans with the two spatially varying parameters (a, b).

Acknowledgment

The author would like to thank the anonymous reviewers for their comments which improved the manuscript a great dea, as well as C. Fan for computational assistance.

References

[1] G. Galanis, P. Louka, P. Katsafados, G. Kallos, and I. Pytharoulis, "Applications of Kalman filters based on non-linear functions to numerical weather predictions," *Ann. Geophys.*, vol. 24, pp. 2451–2460, 2005.
[2] C. J. Lozano, A. R. Robinson, H. G. Arrango, A. Gangopadhyay, Q. Sloan, P. J. Haley, L. Anderson, and W. Leslie, "An interdisciplinary ocean prediction system: Assimilation strategies and structured data models," in *Modern Approaches to Data Assimilation in Ocean Modeling*, P. Malanotte-Rizzoli, Ed. Amsterdam, The Netherlands: Elsevier, 1996, pp. 413–-452.
[3] P. C. Chu, "Probability distribution function of the upper equatorial Pacific current speeds," *Geophys. Res. Lett.*, vol. 35, 2008, 10.1029/2008GL033669.
[4] R. T. Pollard and R. C. Millard, "Comparison between observed and simulated wind-generated inertial oscillations," *Deep Sea Res.*, vol. 17, pp. 795–812, 1970.
[5] A. E. Gill, *Atmosphere-Ocean Dynamics*. San Diego, CA: Academic Press, 1982, 662 pp.
[6] L. M. Ivanov and P. C. Chu, "On stochastic stability of regional ocean models to finite-amplitude perturbations of initial conditions," *Dyn. Atmos. Oceans*, vol. 43, pp. 199–225, 2007a, 10.1016/j.dynatmoce.2007.03.001.
[7] L. M. Ivanov and P. C. Chu, "On stochastic stability of regional ocean models with uncertainty in wind forcing," *Nonlinear Process. Geophys.*, vol. 14, pp. 655–670, 2007b.
[8] N. Johnson, S. Kotz, and N. Balakrishnan, *Continuous Univariate Distributions*. New York: Wiley, 1994, vol. 1, 756 pp.
[9] A. H. Monahan, "The probability distribution of sea surface wind speeds. Part-1: Theory and SeaWinds observations," *J. Clim.*, vol. 19, pp. 497–519, 2006.

Peter C. Chu, photograph and biography not available at the time of publication.